This document was prepared in conjunction with work accomplished under Contract No. DE-AC09-96SR18500 with the U. S. Department of Energy.

DISCLAIMER

WSRC-MS-2005-00557

Key Words:
Eluate
Evaporation
Model

Retention:
Permanent

Tracking No. 10560

Physical Property Modeling of Concentrated Cesium Eluate Solutions

Part I – Derivation of Models

A. S. Choi, R. A. Pierce, T. B. Edwards, T. B. Calloway

SEPTEMBER 2005

WSRC-MS-2005-00557

Physical Property Modeling of Concentrated Cesium Eluate Solutions

Part I – Derivation of Models

A. S. Choi, R. A. Pierce, T. B. Edwards, T. B. Calloway

Savannah River National Laboratory, Aiken, South Carolina, 29808, USA

(Completed September 15, 2005)

Major analytes projected to be present in the Hanford Waste Treatment Plant cesium ion-exchange eluate solutions were identified from the available analytical data collected during radioactive bench-scale runs, and a test matrix of cesium eluate solutions was designed within the bounding concentrations of those analytes. A computer model simulating the semi-batch evaporation of cesium eluate solutions was run in conjunction with a multi-electrolyte aqueous system database to calculate the physical properties of each test matrix solution concentrated to the target endpoints of 80% and 100% saturation. The calculated physical properties were analyzed statistically and fitted into mathematical expressions for the bulk solubility, density, viscosity, heat capacity and volume reduction factor as a function of temperature and concentration of each major analyte in the eluate feed. The R^2 of the resulting physical property models ranged from 0.89 to 0.99.

Introduction

The Waste Treatment Plant (WTP) for the River Protection Project at the U.S. Department of Energy's Hanford site is being built to extract radioisotopes from the vast inventory of tank waste and immobilize them in a silicate glass matrix for eventual disposal at a geological repository. The baseline flowsheet for the pretreatment of supernatant liquid wastes includes removal of cesium using regenerative ion-exchange resins [1]. The loaded columns are eluted with nitric acid nominally at 0.5 molar, and the resulting eluate solution containing cesium is concentrated in a forced-convection evaporator to reduce the storage volume and to recover the acid for reuse [2]. The evaporator pot is charged initially with a concentrated HNO_3 solution and kept under a controlled vacuum during feeding so the pot contents would boil at 50 ^oC. The liquid level in the pot is maintained constant by controlling both the feed and boil-up rates. The feeding is continued with no bottom removal until the solution in the pot reaches the target endpoint of 80% saturation with any major salt species present.

One of the critical operating requirements of the eluate evaporator is that the potential for any solids formation in the bottom product must be precluded. To ensure solids-free operation, the bulk solubility of eluate solutions must be determined accurately, and the target evaporation endpoint is to be set at 80% saturation [2]. Operation of the eluate evaporator must also be robust, since sampling capabilities are not built into the evaporator design. Therefore, there is a clear need for tools that can be used to accurately predict the physical properties of concentrated eluate solutions, including the bulk solubility. Such *a priori* predictive tools or models encompassing all waste envelopes would not only provide necessary data for the design and operation of the eluate evaporator and its storage tanks, but supplement or even replace costly bench-scale tests. Thus, the overall scope of this work consisted of two parts; (1) to develop the physical property models of concentrated cesium eluate solutions using the "virtual" data generated from statistically designed computer experiments, and (2) to conduct bench-scale evaporation tests to generate the "actual" data for the validation of those models. This paper addresses Part I, development of the physical property models.

Approach

The physical properties of interest to this work included the bulk solubility, density, viscosity and heat capacity of cesium eluate solutions as a function of temperature and major analyte concentrations. In addition, the volume reduction factor (VRF), defined as the ratio of cumulative eluate volume fed at 80% saturation to that of the initial acid charge to the pot, is needed for proper equipment sizing. The overall approach taken to develop physical property models is broken down into the following six steps:

- Identification of major analytes present in the radioactive cesium eluate samples and their bounding concentrations;
- Design of a test matrix for computer experiments within the bounding concentrations of the major analytes and temperatures between 20 and 60 ^oC;

- Development of a computer model of semi-batch evaporation process;
- Fine-tuning of the thermodynamic database for the nitric-acid based multi-electrolyte systems;
- Calculation of physical properties at 80% and 100% bulk saturation for each matrix solution;
- Derivation of mathematical correlations that best fit calculated physical properties as a function of temperature and major analyte concentrations in the feed.

In essence, this paper is a summary of the results from each of these six task steps. Since the physical property models will be developed using the "virtual" data, they must then be validated against the "actual" test data to establish any credibility for the models. The results of validation and subsequent application of the validated physical property models will be the subject of Part II of this work.

Results and Discussion

The results from each task step are discussed next along with the assumptions made in this work.

Identification of Major Analytes

Available analytical data for the radioactive cesium eluate samples are given in Table 1 [3]. They were collected during small-scale ion-exchange (IX) tests at both Savannah River National Laboratory (SRNL) and Pacific Northwest National Laboratory (PNNL) using the actual Hanford supernate samples from Tanks AN-102, AN-103, AN-105, AN-107 and AZ-102. Since the degree of salt dilution that occurred during the elution and resin-reconditioning cycles was not the same in all tests, the data given in Table 1 reflect the re-normalization of the respective raw data to a constant 13 column-volume elution. However, missing from this table is the concentration of hydronium ion, or H^+, which is the most dominant species on a molar basis but was not measured routinely during bench-scale tests. Therefore, it was

Table 1. Analytical Data for Cesium Eluate Samples Used in Test Matrix Development.

Sample ID Data Source	AN-103 SRNL	AN-102 SRNL	AZ-102 SRNL	AN-105 SRNL	AN-107 SRNL	AW-101 PNNL	AN-107 PNNL
Cs (uCi/mL)	2500	511	10523	1938	998	3220	365
Cs (ug/mL)	115	24	485	89	46	148	4
ICP-ES (mg/L)							
Na	1060	1480	1626	6246	931	4460	708
Al	59	268	4	614	30	282	3
Si	<1	98	<1	33	16	104	12
Cr	15	10	42	37	8	7	4
Ni	<19	4.5	<1	2	35	6	68
Pb	<81	<9.3	<2	14	9	10	8
Ca	290	66	9	86	10	4	<3
Cu	8	30	<1	6	16	102	15
Fe	12	7	4	4	63	24	5
Mg	13	9	<1	9	3	<1	<1
Zn	21	4	<1	<1	2	24	<1
B	<1	223	<1	45	39	<1	<1
U	322	17	15	17	203	96	67
K (AA)	72	80	107	296	33	764	16
Carbon (mg/L)							
TOC	940	470	267	10769	9308	240	116
TIC	188	<21	324	222	169		
IC (mg/L)							
NO3-	19000	22400	21300	26500	28200	33000	24500
NO2-			952				
Cl- (by IC)	8300						
Cl- (by ISE)		<22	292	293		<100	<2
PO4(3-)			<100			18	
Calculated Results							
H+ (mg/L)	241	280	289	81	404	292	363
wt% total solids	2.14	2.58	2.47	3.40	3.00	3.97	2.58

estimated by charge balancing all reported cation data above detection limits against the nitrate/nitrite data. The reason for excluding the remaining anions and total inorganic carbon (TIC) from the charge balance was because most of their reported values were either near the detection limits or at least two orders of magnitude lower than that of the dominant nitrate.

Despite consistently higher reported values than TIC and other minor anions, the total organic carbon (TOC) data were also excluded from the charge balance for two reasons. First, those exceptionally high TOC values for AN-105 and AN-107 (SRNL) samples were ignored, because they were attributed to the residual organic byproducts from the resin manufacturing process; they did not show up in later samples when the new resin produced with improved pretreatment technique was used. Second, there was no information or data available that could be used to infer the chemical makeup of the TOC data. As a result, ten likely candidate species were selected to study the effects of organics on the eluate solubility [3]: 1) formate, 2) citrate, 3) gluconate, 4) glycolate, 5) tributylphophate (TBP), 6) n-paraffin hydrocarbon (NPH), 7) acetate, 8) oxalate, 9) dibutylphosphate (DBP), 10) ethylenediaminetetraacetic acid (EDTA). However, most of these organic compounds selected were determined to have little or no effect on the eluate solubility due to their volatility or reactivity with nitric acid. For example, formate is oxidized by strong nitric acid to form carbon dioxide and water [4]. Citrate, gluconate, and glycolate are expected to react with nitric acid to form oxalate [5]. Studies at SRNL have shown that both TBP and NPH readily steam strip to less than 1 mg/L [6], and acetic acid is significantly more volatile than either TBP or NPH. The remaining candidate species (oxalate, DBP, and EDTA) were determined experimentally to have some impact on the eluate solubility [7]. However, it was concluded that these species are not present in high enough concentrations to be of concern.

The concentrations of H^+ thus estimated from the charge balance are shown in Table 1, ranging from 0.24 to 0.40 M, except for the AN-105 sample. The low acidity of that sample was the direct result of an abnormally high concentration of sodium ion, which could very well have been due to analytical errors. For this reason, the AN-105 data set was deleted from further considerations. Once the acidity of each eluate sample was estimated, the major and minor species to be considered in the computer test matrix were determined next, as shown in Table 2. The six major cation species chosen were Na^+, H^+, Cs^+, K^+, Al^{+3}, and Ca^{+2} in the order of decreasing average weight fractions and, along with temperature, they constituted the seven computer test matrix variables. Seven minor cation species were also added to the test matrix but only as the background group, and their concentrations were fixed at their respective average values of the six data sets.

Table 2. Major and Minor Species Selected for Computer Test Matrix.

Sample ID Data Source	AN-103 SRNL	AN-102 SRNL	AZ-102 SRNL	AN-107 SRNL	AW-101 PNNL	AN-107 PNNL	Avg All Data	Min All Data	Max All Data
Major Cations									
Cs (wt%)	6.03	1.06	18.90	2.89	2.42	0.34	5.27	0.34	18.90
K	3.78	3.54	4.17	2.08	12.48	1.34	4.56	1.34	12.48
Na	55.62	65.42	63.36	58.57	72.84	59.31	62.52	55.62	72.84
Al	3.10	11.85	0.16	1.89	4.61	0.25	3.64	0.16	11.85
Ca	15.22	2.92	0.35	0.63	0.07	0.00	3.20	0.00	15.22
H+	12.64	12.37	11.28	25.39	4.77	30.39	16.14	4.77	30.39
Minor Cations									
Cr (wt%)	0.79	0.44	1.64	0.50	0.11	0.34	0.64	0.11	1.64
Ni	0.00	0.20	0.00	2.20	0.10	5.70	1.37	0.00	5.70
Pb	0.00	0.00	0.00	0.57	0.16	0.67	0.23	0.00	0.67
Cu	0.42	1.33	0.00	1.01	1.67	1.26	0.95	0.00	1.67
Fe	0.63	0.31	0.16	3.96	0.39	0.42	0.98	0.16	3.96
Mg	0.68	0.40	0.00	0.19	0.00	0.00	0.21	0.00	0.68
Zn	1.10	0.18	0.00	0.13	0.39	0.00	0.30	0.00	1.10
total (wt%)	100.00	100.00	100.00	100.00	100.00	100.00			
total (major)	96.38	97.15	98.21	91.44	97.17	91.62	95.33		
total (minor)	3.62	2.85	1.79	8.56	2.83	8.38	4.67		
wt% total solids	2.14	2.58	2.47	3.00	3.97	2.58	2.79		

Therefore, the minor cations together made up for 4.67 wt% of the total cations in each test matrix solution and the concentrations of the six major cations were varied within their maximum and minimum bounds to account for the remaining 95.33 wt%. Nitrate was the only counterbalancing anion chosen since its concentration far exceeded those of all the remaining anions combined. Furthermore, although present at concentrations above detection limits, uranium, silica and boron were not included as part of the minor cation group based on the following observations:

- The concentration of uranium would have been much lower than those given in Table 1 had the supernate feeds gone through the precipitation step prior to the cesium ion-exchange to remove strontium and transuranic, as the WTP flowsheet prescribes [2].
- The presence of silica and boron was attributed to the leaching of glassware during the storage of strongly acidic samples.

In Table 2, the cation concentrations are given in weight percent of the total cations only, instead of the more conventional wet-basis units such as molar. The reason for using the dry-basis unit is to avoid having multiple physical property predictions for the same saturated solution. For instance, if two feeds have the same composition on a dry basis but differ in water content, boiling of these feeds will lead to the same saturated solution, provided water is the only volatile species. However, the models derived as a function of wet-basis feed composition will predict different physical properties for the same solution. In the case of cesium eluate evaporation, both water and nitric acid will be volatilizing. However, the potential for multiple physical property predictions still exists, if the concentrations of nitric acid in the bottom and overhead stream closely follow the same vapor-liquid equilibrium curve for the multi-electrolyte system.

Design of Test Matrix

The test matrix defines the necessary data points where physical properties need to be calculated using the computer model. The number of necessary data points is determined by both the number of variables or factors in the matrix and the mathematical form of a particular physical property model to be fitted. The minimum and maximum concentration ranges of the six major cations given in Table 2 along with the temperature range between 20 and 60 ^{o}C formed the factor space of interest for the test matrix design. However, there were two challenges that had to be addressed. The first of these revolved around the fact that the sum of the concentrations of the six major cations at each design point was fixed at their average value of 95.33 wt%. Thus, the amounts of those six cations formed a mixture and, as a consequence, the candidate response models were mixture models [8]. The temperature factor introduced as a process variable further complicated the candidate mixture models. The second challenge was to find the space-filling design that would provide a thorough coverage of the factor space [9]. The mixture aspect of this problem prevented a straight-forward application of the space-filling design.

The approach taken to generate a set of design points for this problem was one that is often used in generating a test matrix for statistical experiments; to select a test matrix covering the factor space and satisfying all the constraints, including the mixture constraint, that is optimal relative to one of the several criteria that are all model dependent. For this problem, the following linear mixture model with a process variable was selected as the model to be fitted to each of the responses of interest:

$$\begin{aligned}\text{Response}_{\text{model}} = {} & \beta_1 \cdot Al + \beta_2 \cdot Ca + \beta_3 \cdot Cs + \beta_4 \cdot H + \beta_5 \cdot K \\ & + \beta_6 \cdot Na + \beta_7 \cdot Al \cdot Temp + \beta_8 \cdot Ca \cdot Temp \\ & + \beta_9 \cdot Cs \cdot Temp + \beta_{10} \cdot H \cdot Temp + \beta_{11} \cdot K \cdot Temp \\ & + \beta_{12} \cdot Na \cdot Temp\end{aligned}$$

where the concentration of each cation is in weight fraction, and β's are the coefficients. This model has a total of 12 coefficients, thus requiring at least 12 computer model runs to generate the necessary data to fit the linear mixture model in the concentration factors with and without the temperature factor. To support these first test phase (Phase 1) runs, 6 design points were selected using the D-optimal routine of JMP® software [10]. These 6 design points were run at both the upper and lower temperature bounds for a total of 12 design points in all, as shown in Table 3.

Table 3.Phase 1 Test Matrix Points for Computer Model Runs (in Scaled Weight Fractions).

Run ID	Al (SWF)	Ca (SWF)	Cs (SWF)	H (SWF)	K (SWF)	Na (SWF)	T (^{o}C)
1	0.11065	0.15970	0.08215	0.05000	0.01410	0.58340	20
2	0.03306	0.00000	0.00360	0.31880	0.01410	0.63044	20
3	0.00170	0.15970	0.00360	0.12070	0.13090	0.58340	20
4	0.00170	0.15970	0.01040	0.05000	0.01410	0.76410	20
5	0.00170	0.00000	0.19830	0.05000	0.13090	0.61910	20
6	0.12430	0.00000	0.00360	0.05000	0.05800	0.76410	20
7	0.11065	0.15970	0.08215	0.05000	0.01410	0.58340	60
8	0.03306	0.00000	0.00360	0.31880	0.01410	0.63044	60
9	0.00170	0.15970	0.00360	0.12070	0.13090	0.58340	60
10	0.00170	0.15970	0.01040	0.05000	0.01410	0.76410	60
11	0.00170	0.00000	0.19830	0.05000	0.13090	0.61910	60
12	0.12430	0.00000	0.00360	0.05000	0.05800	0.76410	60

If the 12 coefficients of each physical property model could be fitted well with the data generated from Phase 1, the performance of these linear models was to be evaluated against the "virtual experimental data" generated during the second test phase (Phase 2) runs using the 31 Orthogonal Latin Hypercube (OLH) design points shown in Table 4 [11]. Again, the mixture constraint limited the effectiveness of the OLH approach in filling in the factor space, and Figure 1 shows the resulting "space-filling" achieved after two successive OLH runs.

Table 4. Phase 2 OLH Design Points for Computer Model Runs (in Scaled Weight Fractions).

Run ID	Al (SWF)	Ca (SWF)	Cs (SWF)	H (SWF)	K (SWF)	Na (SWF)	T (^oC)
13	0.06682	0.06985	0.07658	0.16003	0.04327	0.58345	59
14	0.07066	0.08482	0.08266	0.12585	0.04692	0.58909	20
15	0.07449	0.05987	0.11308	0.10725	0.05057	0.59474	24
16	0.07832	0.09480	0.10700	0.06528	0.05423	0.60038	57.5
17	0.08215	0.04989	0.05224	0.12260	0.08709	0.60603	54
18	0.08598	0.10477	0.05832	0.05581	0.08344	0.61167	25
19	0.09748	0.02994	0.02790	0.11170	0.01406	0.71892	49
20	0.11281	0.00998	0.00357	0.06100	0.11631	0.69634	44
21	0.03234	0.04490	0.07049	0.05887	0.06883	0.72457	27.5
22	0.01701	0.02495	0.04616	0.14639	0.11996	0.64554	32.5
23	0.00934	0.01497	0.19217	0.09437	0.03232	0.65683	45
24	0.00551	0.15966	0.01573	0.12066	0.03597	0.66248	41
25	0.00168	0.00499	0.02182	0.26377	0.03962	0.66812	37.5
26	0.05380	0.05588	0.06199	0.12670	0.05498	0.64665	59
27	0.05687	0.06785	0.06686	0.08448	0.06374	0.66020	20
28	0.05993	0.04790	0.09119	0.11423	0.04914	0.63761	24
29	0.06606	0.03991	0.04253	0.17962	0.04330	0.62857	54
30	0.07219	0.03193	0.11066	0.12822	0.03746	0.61954	29
31	0.07832	0.02395	0.02306	0.23254	0.03162	0.61051	49
32	0.08446	0.01597	0.13012	0.14221	0.02578	0.60147	34
33	0.09058	0.00798	0.00360	0.28546	0.01994	0.59244	44
34	0.09671	0.00000	0.14959	0.15620	0.01410	0.58340	39
35	0.05074	0.06386	0.08146	0.08744	0.06082	0.65568	40
36	0.04461	0.05987	0.09606	0.09040	0.05790	0.65116	60
37	0.04154	0.07983	0.07173	0.06065	0.07250	0.67375	56
38	0.03848	0.05189	0.07659	0.13885	0.05206	0.64213	22.5
39	0.03235	0.04390	0.11552	0.12891	0.04622	0.63309	55
40	0.02622	0.03592	0.05713	0.21629	0.04038	0.62406	27.5
41	0.02009	0.02794	0.13499	0.16742	0.03454	0.61502	50
42	0.01396	0.01996	0.03766	0.29373	0.02870	0.60599	32.5
43	0.00783	0.01197	0.15445	0.20593	0.02286	0.59695	45

Process Modeling

Each cycle of the semi-batch evaporation process to be modeled begins by charging the evaporator pot with a concentrated HNO_3 solution (~7.5 M) before the commencement of feeding. The pot is kept under vacuum so that boilup would occur at ~50 ^oC. The cesium eluate is then fed to the pot while maintaining a constant liquid level in the pot. The feeding and boilup will continue with no bottom withdrawal until the pot contents reaches the target endpoint of 80% saturation with respect to any major salt species present. As the feeding and boilup continue, the acid content in the pot will continue to decrease, while its salt content continues to increase. As a result, the vapor-liquid equilibrium (VLE) of the HNO_3 solution

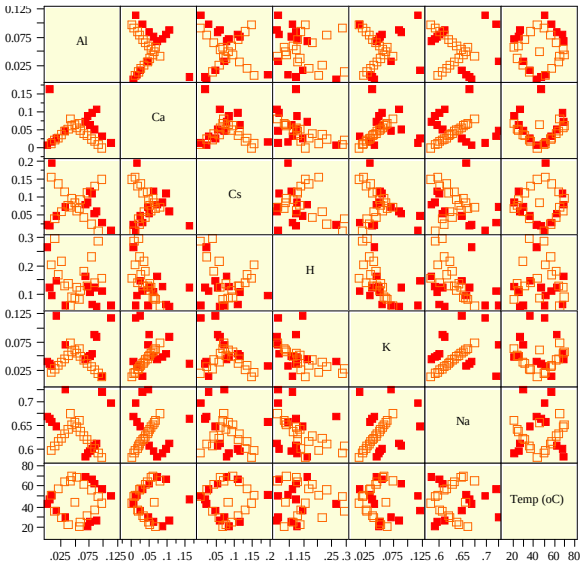

Figure 1. Scatter Plots of Phase 1 (•) and Phase 2 (•) Design Points Using OLH Approach.

will also vary constantly. The aqueous chemistry of this evaporation process was modeled using the Environmental Simulation Program (ESP) [12].

Since the ESP software is a steady state process simulator, the semi-batch evaporation process was approximated by a series of continuous still pots, as shown in Figure 2. The mass ratio of the initial acid charge-to-eluate feed to the 1st stage was set at 5:1. Additional stages were then added to the model one-by-one at the bottom-to-feed ratio of 5:1, until the bottom product from the final stage reaches the target endpoint of 80% saturation at 25 ^oC and 1 atm. Higher mass ratios of 10:1 and 100:1 were also tried and found to have little impact on the overall VLE; they only affected the number of stages required for a given target endpoint. The validity of approximating the semi-batch evaporator as a series of continuous still pots was confirmed earlier against the batch distillation data collected at 1 atm [13].

One of the key process constraints to be met during the execution of the model is to maintain the liquid level in the pot constant throughout boilup, which is equivalent to maintaining a constant flow of concentrate from one stage to the next in the current modeling scheme. It turned out that by maintaining the molar boilup rate very close to that of the feed and letting the pot vacuum float, it was possible to contain the volume fluctuations within ±2%. The concentration of initial acid charge was set at 7.25 M, since its equilibrium vapor concentration at 50 ^oC is ~0.5 M, which is the target acidity for the condensate for reuse during the next IX column elution cycle.

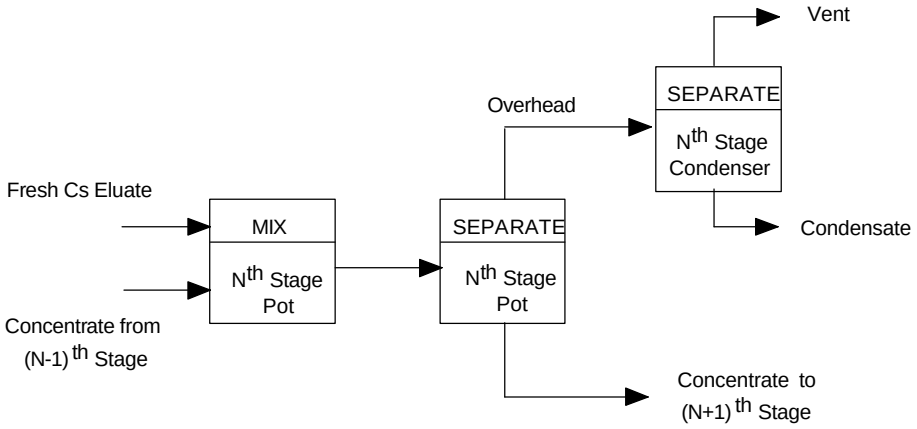

Figure 2. Schematic of Nth Stage Semi-Batch Evaporation of Cs Eluate.

Furthermore, the bulk saturation point of a multi-electrolyte system was defined as the point where the solution would become just saturated with any of the major salt species present or supersaturated with the remaining minor salt species to the extent that the total insoluble solids formed exclusively out of the minor salt constituents would exceed 0.5 wt% of the solution, whichever occurs first. These criteria were applied to the projected eluate storage conditions of 25 ^{o}C and 1 atm. Experimentally, the determination of 0.5 wt% minor salt species-only presence will require both quantification and phase identification of filtered solids from a few samples taken beyond the formation of first solids. Once the bulk saturation limit was determined for each matrix solution, the 80% saturation endpoint was determined as the point where the ionic product of the target salt constituents equaled 80% of its solubility product.

Database

The accuracy of model predictions such as the first salt species to precipitate and its solubility limit depends entirely on the accuracy of thermodynamic database(s) used. Every ESP model is built to run in conjunction with the ESP software's default database called PUBLIC. In this work, the PUBLIC database v6.5 was supplemented by a private database, called HNO3DB (also referred to as the nitric acid database, hereafter), since the former alone did not adequately predict the observed vapor-liquid and solid-liquid equilibria for nitrated systems under strongly acidic conditions. The nitric acid database was developed in stages, starting from the simple HNO_3-H_2O binary system to the final Na-K-Cs-Al-HNO_3-H_2O sexenary system by adding the nitrated salts of Na, K, Cs, and Al one by one. In Figure 3, the calculated equilibrium pressures of the HNO_3-H_2O binary system using the re-optimized binary HNO3DB up to the azeotrope are compared against the measured values [14], and the overall agreement is seen to be quite good.

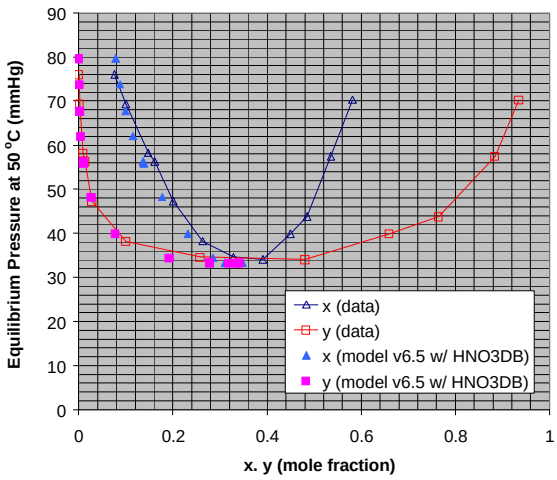

Figure 3. Calculated vs. Measured Equilibrium Pressures of HNO_3-H_2O System at 50 ^{o}C.

The next step taken in the database development was to predict ternary system properties involving three alkali salts using the binary HNO3DB, and the outcome was not satisfactory. This means that the binary interaction parameters for Na^+, K^+, Cs^+, and their undissociated salts had to be re-optimized, and the binary and ternary data that were regressed were assembled from two different sources: SRNL bench-scale tests (~35%) and the open literature (~65%). The optimization led to the expanded HNO3DB for the Na-K-Cs-HNO_3-H_2O quinary system. Solubilities and saturation densities of the three ternary systems, (Na,K,Cs)-HNO_3-H_2O, were then re-calculated using the quinary HNO3DB, and significant improvements were seen over the binary HNO3DB predictions [15].

Finally, the quinary HNO3DB was optimized further by including Al, and the resulting sexenary HNO3DB for the Na-K-Cs-Al-HNO_3-H_2O system included every binary interaction possible among all major cations selected for the test matrix, except for Ca^{+2}; inclusion of Ca^{+2} was not possible due to lack of data. A brief account of the bench-scale tests performed at SRNL to generate the solubility data for ternary and higher-order systems is given next.

Ternary Solubility Data

To provide the necessary ternary solubility data for the regression, a matrix of alkali solutions was prepared with increasing concentrations of $NaNO_3$, KNO_3 and $CsNO_3$ at several fixed concentrations of HNO_3. Solids were weighed on a calibrated balance accurate to 0.0001 g. Nitric acid (15.7 M) was added using a calibrated pipette. The mixture was prepared at room temperature in a 25-cm^3 volumetric flask, and deionized water was added until the total volume reached the mark on the volumetric flask. All solids added were allowed to dissolve and, as needed, water was added to the flask to make up for any volume loss accompanying the dissolution of solids.

The samples were analyzed using an Anton-Paar DMA 4500 density meter, which is accurate to 0.0001 g/cm^3. Prior to analyzing samples, instrument calibration was verified using deionized water, and additional checks were performed using a 28 wt% $NaNO_3$ solution. Samples were injected into the instrument, and the sample temperature was adjusted to 20 ^oC before analysis. Using the ternary system density data, it was possible to obtain approximate solubility limits at 20 ^oC for the corresponding salt-HNO_3-H_2O systems. The density data were plotted as a function of salt concentrations at a given HNO_3 concentration. The data yielded linear plots for the under-saturated ternary solutions, which were then extrapolated to the saturation density and the corresponding saturation molarity was determined for each salt-HNO_3-H_2O ternary system. The estimated solubility data based on the linear extrapolations are listed in Table 5 [7].

Table 5. Ternary Solubility Limits Measured at SRNL.

HNO_3 (M)	$NaNO_3$ (M)	KNO_3 (M)	$CsNO_3$ (M)
0	7.31	2.93	1.16
3	----	1.83	0.78
4	3.52	1.43	0.80
5	----	1.60	1.00
6	2.27	1.55	1.09
8	1.56	----	----

Furthermore, an excellent agreement shown in Figure 4 between the measured saturation densities of the $NaNO_3$-H_2O system at 20 ^oC and those found in the literature confirms the validity of experimental techniques used by the SRNL personnel. All physical property data measured for the entire matrix of ternary samples are documented elsewhere [7].

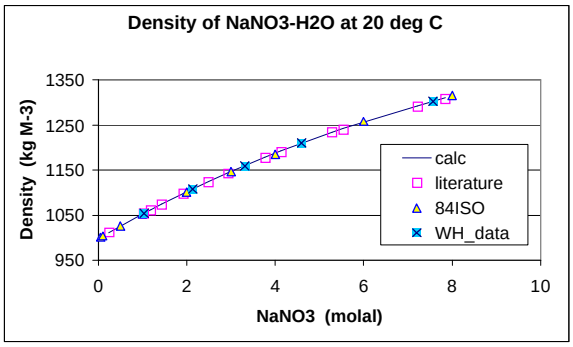

Figure 4. Comparison of SRNL and Literature Data.

Multi-Component Solubility Data

A matrix of solids mixtures was prepared that contained a total of nine cations, of which six were allowed to vary. To evaluate the effects of various salts on the bulk solubility, the relative salt ratios in the matrix were set to represent those observed in the cesium eluate samples from ion-exchange tests using actual tank waste as well as those ratios proposed as part of the statistically-designed matrix [3,7]. For each matrix sample, appropriate salts were individually weighed on a calibrated balance and added to a sample bottle. The solids were then ground and blended to create a uniform mixture.

To determine the ambient-temperature solubility (20±2 ^oC) at varying acid concentrations, a known volume and concentration of HNO_3 (3 to 5 M) was added to the test vessel which was set up on a stirrer. The vessel was sealed and the acid was stirred at atmospheric pressure. Periodically, the solids from the matrix batches were incrementally added to the vessel and allowed to dissolve. The solubility limit was identified as the point where the solids did not dissolve after 30 minutes in contact with the acid. Once any undissolved solids were first observed, they were allowed to settle overnight. The supernatant liquid sample was then withdrawn from the top and analyzed for density, viscosity, and heat capacity. Some of the results obtained from the statistically-designed matrix tests are listed in Table 6 [7]. The compositions of the listed cesium eluate simulants are given in Table 1.

Table 6. Physical Properties of Multi-component Solutions at Saturation.

Matrix	Starting [HNO_3] (M)	Density at 20 °C (g/cm^3)	Heat Cap. at 50 °C (cal/g-C)	Viscosity at 50 °C (cP)
AZ-102	3	1.380	0.667	1.38
AZ-102	4	1.375	0.657	1.28
AZ-102	5	1.365	0.670	1.27
AN-102	3	1.369	0.662	1.96
AN-102	4	1.363	0.667	1.66
AN-102	5	1.369	0.665	1.88
AN-103	3	1.413	0.651	2.10
AN-103	4	1.397	0.653	1.93
AN-103	5	1.392	0.620	1.66
AN-107	3	1.350	0.676	1.37
AN-107	4	1.352	0.684	1.41
AN-107	5	1.341	0.682	1.23
AN-105	3	1.357	0.674	1.56
AN-105	4	1.345	0.686	1.38
AN-105	5	1.341	0.686	1.46

Before the sexenary HNO3DB for the Na-K-Cs-Al-HNO_3-H_2O system was put to use in calculating the physical properties of the test matrix solutions, it was tested against the data from additional bench-scale tests conducted at SRNL with the Tank AZ-102 TFL cesium eluate simulant at two different starting acidities of 7.25 and 8.56 M [16]. The ESP model was run with the sexenary HNO3DB to simulate the test conditions, and the resulting model predictions are compared in Table 7 against the data. Here, the volume reduction factor (VRF) is defined as the ratio of cumulative feed volume to that of the initial acid charge. The results of additional validation efforts are given in Table 8 using the bench-scale data from the AN-102 and AZ-102 eluate simulant runs. It is shown that all these model predictions matched the corresponding data well within ±15%, thus satisfying the specified acceptance criterion for this work.

Table 7. Validation of Sexenary HNO3DB against AZ-102 TFL Data.

Initial Acidity (M)	Parameters @ Saturation	Data	Model
7.25	VRF	42-56	51
	Density (g/ml)	1.3508[a]	1.3343
	Acidity (M)	4.86[a]	4.32
	Cumulative Condensate Acidity	0.595[a]	0.57
	Boiling Point at 70 torr (°C)	55-58	55
8.56	VRF	51-55	51
	Density @ VRF = 50 (g/ml)	1.3372	1.3344
	Acidity @ Saturation (M)	4.81[a]	4.32
	Cumulative Condensate Acidity	0.55[a]	0.59

[a] measured at the highest VRF

Table 8. Validation of Sexenary HNO3DB against AZ-102 and AN-102 Data.

Cs eluate		Data	Model	% diff [a]
AZ-102	Density (g/ml)	1.3531	1.3610	2.2
	Solubility (g TS/ml)[b]	0.6067	0.6290	3.7
AN-102	Density (g/ml)	1.3676	1.3444	6.3
	Solubility (g TS/ml)[b]	0.6160	0.5770	6.5

[a] Based on decimals only; [b] TS stands for total solids.

Calculation of Physical Properties

The ESP semi-batch evaporation model was run with the sexenary HNO3DB to calculate the physical properties of 43 matrix solutions at 80% and 100% saturation. It turned out that the first-precipitating major salt species was always $NaNO_3$ for all matrix solutions. Therefore, the model was run with each matrix feed, until the ionic product of Na^+ and NO_3^- equaled the solubility product of $NaNO_3$. Once the bulk solubility limit was calculated for each matrix feed, the 80% saturation target was found by backing off to the point where the ionic product of Na^+ and NO_3^- equaled 80% of its solubility product. The density, viscosity and heat capacity of the 100% and 80% saturated solutions were then calculated along with the VRF, sometimes called the concentration factor. The achievable VRF at a given target endpoint should be useful to the design of an evaporator and its storage system. The physical property data thus calculated for all 43 matrix solutions are documented elsewhere [15].

Typical evaporation profiles are shown in Figure 6 for Matrix Feed #22 as an example. Throughout the boilup the acidity of the pot decreased steadily from its initial value of 7.25 M to 1.85 M, when the pot became just saturated with $NaNO_3$. The saturation occurred at the 420th evaporation stage of the model (see Figure 1 for the definition of a stage) or at the estimated VRF of 76, which is equivalent to saying, "the pot became saturated with $NaNO_3$ when the total volume of eluate fed equaled 76 times the initial acid volume." If the actual cesium eluate feed had the same composition as that of Matrix Feed #22, the pot would reach the operating target of 80% saturation at the estimated VRF of 57, and the feeding would be terminated at that point.

It is also noted in Figure 6 that the concentration of Na^+ in the pot increased linearly from zero initially to ~4.9 M at 100% saturation, and this linear increase was expected since both the feed rate and the volume of liquid in the pot were kept constant. Also worth noting is that the predicted pot acidity of 1.85 M at

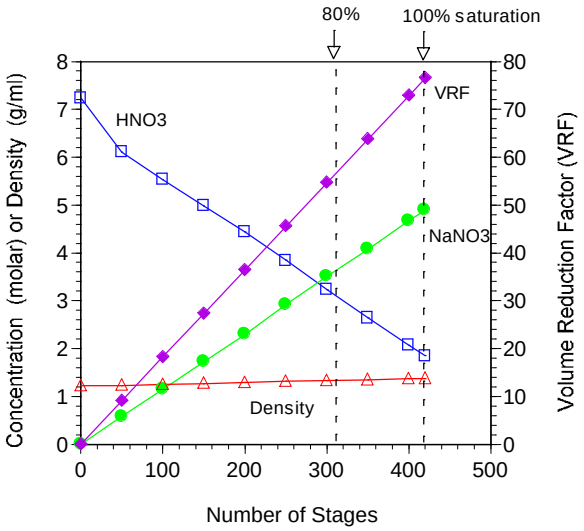

Figure 6. Evaporation Profiles of Matrix Feed #22.

100% saturation is ~2.5X lower than either the predicted or measured acidities of the Tank AZ-102 TFL eluate at the same initial pot acidity of 7.25 M (Table 7). This large discrepancy in the final acidity can be attributed to the differences in both the Na^+ and H^+ concentrations of the two feeds, whose full compositions are compared in Table 9 along with the maximum and minimum bounds of the test matrix. Clearly, the scaled weight fraction of Na^+ in Tank AZ-102 TFL eluate was higher than its counterpart in Matrix Feed #22, which would make the pot saturate more quickly with the former feed, resulting in a less cumulative loss of HNO_3 into the overhead and thus a

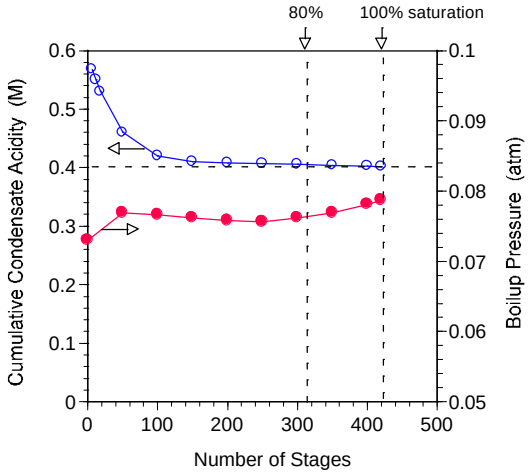

Figure 7. Profiles of Condensate Acidity and Boilup Pressure for Matrix Feed #22.

Derivation of Physical Property Model

higher acidity remaining in the pot. At the same time, the concentration of H^+ in Tank AZ-102 TFL eluate is ~70% higher than its counterpart in Matrix Feed #22, which would make the final acidity remaining in the pot even higher with the former feed. However, it is interesting to note in Table 7 that both the model and the measured data showed that the pot would reach the same acidity at saturation regardless of the initial acidity in the pot.

Table 9. Comparison of AZ-102 TFL and Matrix #22 Feed Compositions.

	AZ-102 TFL (SWF)	Matrix 22 (SWF)	Min (SWF)	Max (SWF)
Al	0.0018	0.0170	0.0017	0.1243
Ca	0.0026	0.0250	0.0000	0.1597
Cs	0.0036	0.0462	0.0036	0.1983
H	0.2497	0.1464	0.0500	0.3188
K	0.0124	0.1200	0.0141	0.1309
Na	0.7299	0.6455	0.5834	0.7641
Total	1.0000	1.0000		

The profiles of cumulative condensate acidity and boilup pressure are shown in Figure 7 for Matrix Feed #22. The cumulative condensate acidity is shown to start out high initially at near 0.6 M due to high initial acidity in the pot and then quickly fell to the asymptotic value of 0.4 M after the 150th stage or VRF = 27. If it were desired to bring acidity back up to 0.5 M for reuse in eluting the IX columns, use of a rectifier column would achieve this easily.

The ESP model results describing the relevant properties for the first two test phases were analyzed using the statistical software package JMP® v4.0.[10] For both 80% and 100% saturation target endpoints, the responses of interest were density, viscosity and heat capacity. In addition, for the 80% saturation case, the VRF was also of interest and, for the 100% saturation case, the solubility expressed as grams of total solids (TS) per 1,000 grams of water or grams of total solids per milliliter was of interest. Due to the enormity of data obtained from the 43 model runs at each endpoint, only the key results are presented and discussed here.

The calculated solubilities, densities and heat capacities of all matrix solutions at 100% saturation are plotted in Figure 8 as a function of the most dominant Na^+ concentration. In these plots, small squares are used to represent the Phase 1 data, while the Phase 2 data are plotted using a combination of "pluses" and solid circles of different colors depending on the temperature (red for 20 ºC and

green for 60 ºC). In general, a random scatter of data seen in these plots suggests that there are no dominating mixture factors or variables whose effects on any of the mixture properties of interest are clearly manifested for the entire matrix ranges considered in this work.

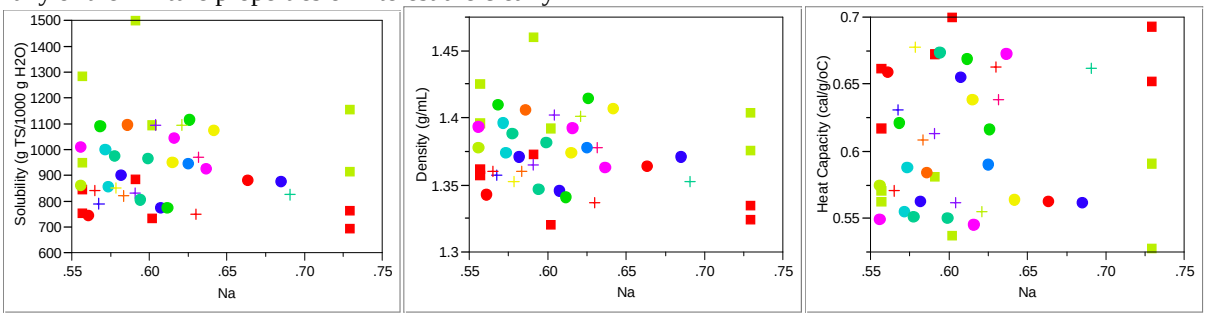

Figure 8. Plots of Calculated Solubilities, Densities and Heat Capacities at 100% Saturation vs. Na^{+} Concentration.

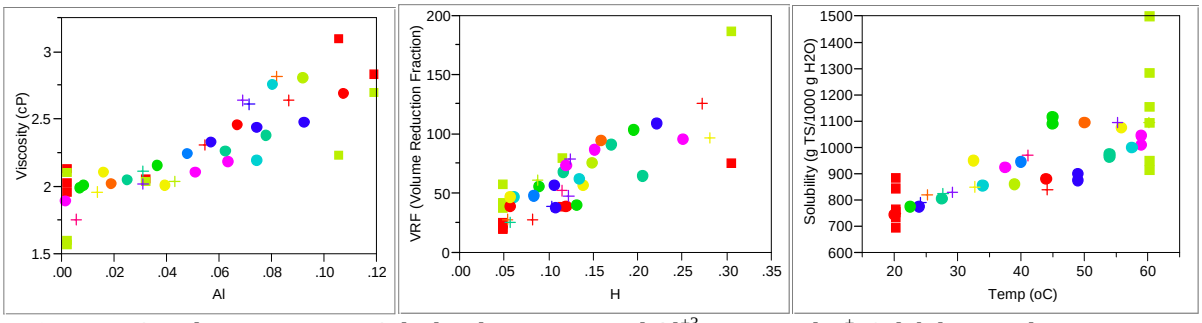

Figure 9. Correlations Between Calculated Viscosites and Al^{+3}, VRFs and H^{+}, Solubilities and Temperature.

However, there were some exceptions to this overall trend; definite correlations are seen in Figure 9 between the viscosity and the concentration of Al^{+3} (at both target endpoints), between the VRF at 80% saturation and the concentration of H^{+}, and between the solubility and temperature. In fact, the effect of temperature was also seen on the density, solubility and, to a lesser degree, the heat capacity.

The first step in the phased approach was to fit a linear mixture model with temperature as a process variable. Since there are 12 Phase-1 data points and 12 model parameters, all of the variation in each set of response data is fully described by the fitted model for that response and, therefore, there are no degrees of freedom remaining for error. To provide some opportunity for improving the performance of these fitted models, a subset of the OLH data points were selected to participate in the model fitting process. Starting with the 15th design point, every third design point was selected to be used in the model fitting (these points are represented by "plus" symbols), while the remaining OLH points continued to be used for model validation (these points are represented by solid circles). These models could explain over 90 and 95% of the variations seen in the 80% and 100% saturation data, respectively.

Since the models based on the expanded data sets appeared to perform well for both the 80% and 100% saturation cases, the last step in the phased approach was to develop a final set of models using all 43 matrix points generated in both test phases.[15] The predicted solubility, viscosity and heat capacity using the resulting response models from the last step are compared in Figure 10 against the corresponding ESP model predictions at saturation. It is recalled that since the response data were not experimentally generated, there are no experimental or random errors in any of the response models developed in this work and, therefore, any difference between the response model predictions and the ESP model results for a given set of factor levels represents a bias in the model. The sensitivity lines at ±15% of the response model predictions provide an opportunity to assess the bias in the models over the points from the OLH design that were not used in the modeling effort.

It is clearly seen in Figure 10 that all response models, except for the viscosity model at 80% saturation, which is not shown here, predicted the

computer-generated data well inside of the ±15% sensitivity lines. Although not shown, the density model performed much better than any of the models shown. This means that the final response models relate the physical property predictions by the ESP model to the concentration and temperature ranges considered in this study without any significant bias. The resulting values of all 12 parameters for each physical property model are tabulated in Table 10.

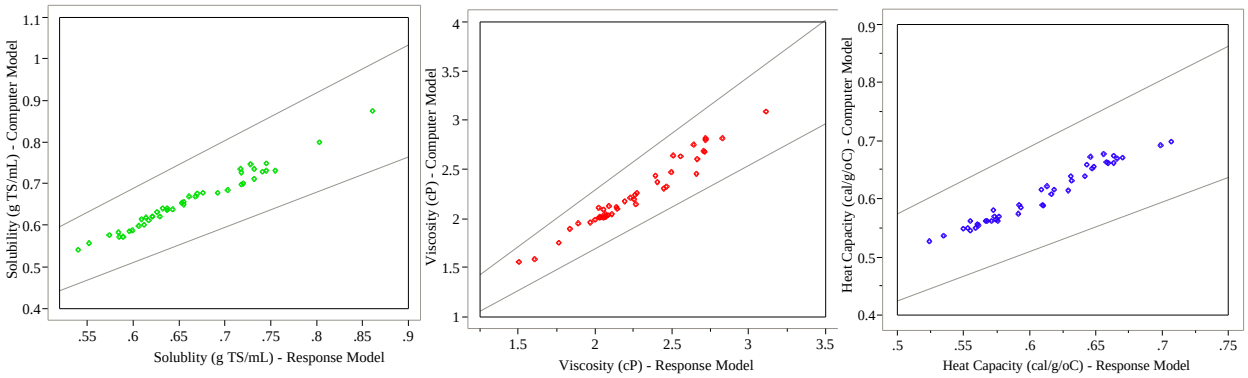

Figure 10. Comparison between Response Model vs. ESP Process Model (Actual) Predictions at 100% Saturation.

Table 10. Coefficients of Physical Property Models Determined by Statistical Analysis Using JMP®.

Coeff.	80% Saturation				100% Saturation			
	Density (g/ml)	**Viscosity (cP)**	**Heat Capacity (cal/g/°C)**	**VRF***	**Density (g/ml)**	**Viscosity (cP)**	**Heat Capacity (cal/g/°C)**	**Solubility (g TS/ml)**
$\bullet_1$	1.36176	6.11135	0.53721	**139.01782**	1.48886	12.72718	-0.03378	0.73699
$\bullet_2$	1.44401	3.03668	0.57243	**48.97029**	1.47408	4.95164	0.38964	0.74161
$\bullet_3$	1.34916	2.26934	0.58492	**27.90272**	1.50460	3.95236	0.49192	0.69789
$\bullet_4$	1.30755	2.94761	0.85864	**63.09169**	1.31406	2.14149	0.84166	0.51292
$\bullet_5$	1.37269	1.59566	0.59123	**54.90814**	1.42237	2.51310	0.46440	0.77862
$\bullet_6$	1.24086	1.66923	0.78125	**-11.80459**	1.25453	1.38919	0.83926	0.42178
$\bullet_7$	-0.00244	0.03731	-0.01159	**-3.30647**	-0.00619	-0.07447	0.00287	-0.01693
$\bullet_8$	-0.00162	-0.04848	0.00036	**-1.07174**	-0.00111	-0.09208	0.00499	-0.00097
$\bullet_9$	0.00389	0.00220	0.00178	**0.58164**	0.00147	-0.02821	0.00185	0.00599
$\bullet_{10}$	0.00061	-0.03509	-0.00621	**7.73972**	0.00142	-0.00294	-0.00599	0.00356
$\bullet_{11}$	0.00270	0.02265	-0.00271	**-0.48689**	0.00209	0.00172	0.00039	0.00590
$\bullet_{12}$	0.00217	-0.00210	-0.00213	**0.52935**	0.00240	0.00758	-0.00426	0.00559

Conclusions

The task of developing the physical property models required a coherent plan for multi-faceted execution such as the critical evaluation of analytical data for radioactive cesium eluate samples, continual assessment and improvement of thermodynamic and physical property databases, buildup and execution of computer process models, and finally the statistical design and analysis of computer experiments and response data. The physical property models thus constructed out of the "virtual data" will be validated in Part II against the "real" data from on-going bench-scale tests with simulated multi-electrolyte cesium eluate solutions.

*
This work was conducted at the Savannah River National Laboratory in Aiken, SC, which is operated for the U. S. Department of Energy (DOE) by Westinghouse Savannah River Company under Contract DE-AC09-96SR18500. The Hanford River Protection Project – Waste Treatment Plant (RPP-WTP) funded this work. The authors are very grateful to James Clark for his assistance in the experimental work.

References

1. J. W. OLSON, "System Description for Cesium Removal Using Ion Exchange – System CXP," 24590-PTF-3YD-CXP-00001, Rev. A, Bechtel National, Inc., Richland, WA, 2001.
2. M. WOODWORTH, "System Description for Cesium Nitric Acid Recovery Process – System CNP," 24590-PTF-3YD-CNP-00001, Rev. B, Bechtel National, Inc., Richland, WA, 2002.
3. R. A. PIERCE, "Cesium Eluate Analytical Data Evaluation," WSRC-TR-2001-00594, Westinghouse Savannah River Co., Aiken, SC, 2002.
4. *Kirk-Othmer Encyclopedia of Chemical Technology*, 4th Ed., Vol. 11, *p 953*, John Wiley & Sons, New York, 1994.
5. *Kirk-Othmer Encyclopedia of Chemical Technology*, 4th Ed., Vol. 17, pp 882-886, John Wiley & Sons, New York, 1994.
6. R. A. Pierce, "Stripping of Tributylphosphate (TBP) with Steam During Evaporation," WSRC-TR-2000-00158, Westinghouse Savannah River Co., Aiken, SC, 2000.
7. R. A. PIERCE, T. B. EDWARDS, "Cesium Eluate Evaporation Solubility and Physical Property Behavior," WSRC-TR-2002-00273, Westinghouse Savannah River Co., Aiken, SC, 2002.
8. J. CORNEL, *Experiments with Mixtures: Designs, Models, and the Analysis of Mixture Data*, Third Edition, John Wiley & Sons, Inc., New York, 2002.
9. T. J. SANTER, B. J. WILLIAMS, W. I. NOTZ, *The Design and Analysis of Computer Experiments*, Springer-Verlag New York, Inc., New York, 2003.
10. *JMP® Statistics and Graphics Guide*, Version 4, SAS Institute, Inc., Cary, NC, 2000.
11. K. Q. YE, "Orthogonal Column Latin Hypercubes and Their Application in Computer Experiments," *Journal of the American Statistical Association*, 93, pp 1430-1439, 1998.
12. ESP SOFTWARE, http://www.olisystems.com/, OLI Systems, Inc., Morris Plains, NJ, 2002.
13. A. S. Choi, "Estimation of Physical Properties of AN-107 Cesium and Technetium Eluate Blend," WSCR-TR-2000-00527, Westinghouse Savannah River Co., Aiken, SC, 2001.
14. M. A. YAKIMOV, V. YA. MISHIN, Chisa-Congress, Prague 6th, Vol. 6, *p 543* (1964).
15. A. S. CHOI, T. B. EDWARDS, R. A. PIERCE, "Physical Property Models of Concentrated Cesium Eluate Solutions," WSRC-TR-2002-00424, Westinghouse Savannah River Co., Aiken, SC, 2003.
16. R. A. PIERCE, A. S. Choi, "Cesium Eluate Evaporation Solubility and Physical Property Behavior," WSRC-TR-2002-00411, Westinghouse Savannah River Co., Aiken, SC, 2002.